Cancer Immunol Immunother (2018) 67:299–310
https://doi.org/10.1007/s00262-017-2079-7

ORIGINAL ARTICLE

BRAF peptide vaccine facilitates therapy of murine BRAF-mutant melanoma

Qi Liu[1] · Hongda Zhu[1,2] · Yun Liu[1] · Sara Musetti[1] · Leaf Huang[1]

Received: 15 March 2017 / Accepted: 9 October 2017 / Published online: 1 November 2017

Abstract Approximately, 50% of human melanomas are driven by BRAF mutations, which produce tumors that are highly immunosuppressive and often resistant to vaccine therapy. We introduced lipid-coated calcium phosphate nanoparticles (LCP NPs) as a carrier to efficiently deliver a tumor-specific antigen, the $BRAF^{V600E}$ peptide, to drive dendritic cell (DC) maturation and antigen presentation in C57BL6 mice. The BRAF peptide vaccine elicited a robust, antigen-specific cytotoxic T cell response and potent tumor growth inhibition in a murine BRAF-mutant melanoma model. Advanced BRAF-specific immune response was illustrated by IFN-γ production assay and cytotoxic T lymphocyte (CTL) assay. Remodeling of immunosuppressive modules within the tumor microenvironment further facilitated CTL infiltration. Thus, using LCP NPs to deliver the BRAF peptide vaccine is a promising strategy for the BRAF-mutant melanoma therapy.

Keywords BRAF-mutant melanoma · Peptide vaccine · Immunotherapy · Nanoparticles

Abbreviations

CCL2	C-C Motif chemokine 2
CFSE	Carboxyfluorescein succinimidyl ester
DOPA	Dioleoylphosphatydic acid
DOTAP	(±)-N,N,N-Trimethyl-2,3-bis(z-octadec-9-ene-oyloxy)-1-propanaminium chloride
DSPE-PEG-2000	1,2-Distearoyl-sn-glycero-3-phosphoethanolamine-N-[amino(polyethylene glycol)-2000
DSPE-PEG-NHS	3-(N-succinimidyloxyglutaryl) aminopropyl, polyethyleneglycol-carbamyl-distearoylphosphatidylethanolamine
FAP	Fibroblast activation protein
LCP NP	Lipid-coated calcium phosphate nanoparticle
ODN	Oligodeoxynucleotides
OS	Overall survival
TEM	Transmission electron microscope
Th1	Type 1 T helper
TME	Tumor microenvironment

Introduction

Melanoma is one of the most common forms of skin cancer, with an estimated 76,380 new cases in the USA in 2016 [1]. It accounts for nearly 80% of skin cancer deaths. Despite recent improvements in prevention and early detection, approximately 20% of melanoma patients still die from the disease. Early stage melanoma is curable by surgical resection, but metastasis results in poor prognosis; 5-year survival rates drop from 98 to 17% once melanoma metastasizes. This is largely because metastatic malignancy is refractory to conventional therapies. Hence, new treatment therapies are necessary [2].

Recent advances in immunology and cancer biology, including a better understanding of signaling pathways in

✉ Leaf Huang
leafh@unc.edu

[1] Division of Pharmacoengineering and Molecular Pharmaceutics and Center for Nanotechnology in Drug Delivery, Eshelman School of Pharmacy, University of North Carolina at Chapel Hill, 1315 Kerr Hall, Campus Box 7571, Chapel Hill, NC 27599, USA

[2] School of Food and Biology Engineering, Key Laboratory of Fermentation Engineering (Ministry of Education), Hubei University of Technology, Wuhan 430068, China

cancer progression, have promoted cancer immunotherapy as a new way of halting growth and metastasis [3, 4]. Cancer immunotherapy harnesses the patient's immune system to combat cancers. The therapy primarily depends on tumor-associated antigens, which are overexpressed during malignant tumor cell development. The immune system is manipulated to recognize tumor-associated antigens and raise a specific immune response against the cancer cells. The typical strategy is to generate a large number of antigen-specific T cells to battle the tumor by using cancer vaccines [5].

A clinically significant event in the field was the identification of driver oncogenic mutations in the BRAF gene, which encodes a serine/threonine-protein kinase BRaf [6]. BRAF inhibitors have been largely studied as clinical therapeutics in BRAF-mutant cancers. The major efficacy of BRAF inhibitors results from BRAF/MEK/ERK signaling inhibition. Vemurafenib and dabrafenib are two structurally unrelated BRAF inhibitors that selectively target V600E, a missense mutation in BRAF. These BRAF inhibitors increased disease-free survival and overall survival (OS), leading to their regulatory approval in 2011 and 2013, respectively [7, 8]. Combined inhibition of BRAF and MEK can reduce disease progression risk by 25% and delay development of resistance compared with BRAF inhibition alone, but cannot prevent emergence [9].

Notably, 50% of human melanomas are driven by BRAF mutations, among which $BRAF^{V600E}$ mutation is the major common one, characterized by aggressive growth and a highly immunosuppressive tumor microenvironment (TME). These tumors are often resistant to immune vaccination therapy [10]. Therefore, inducing a BRAF-mutation-specific and potent T cell response to endogenous antigens remains challenging. The murine $BRAF^{V600E}$ mutant peptide (mBRAF 594-602: FGLANEKSI) for the C57Bl/6 haplotype ($H2D^b$) was designed by modifying amino acids at the 5 and 9 positions to increase binding affinity using the Rammensee epitope prediction model [11]. A previous report on type 1-polarized DCs pulsed with affinity-modified $BRAF^{V600E}$ peptide showed antigen-specific CD8 + T cell responses [12], supporting mutated BRAF as a potential immune system target. However, cell-based vaccination is both costly and less reproducible compared with an injectable chemical dosage of nano-formulation for targeted delivery to the draining LNs. In this study, we aimed to use a BRAF-mutant melanoma in a syngeneic mouse model to study tumor growth inhibition using a tumor-specific BRAF peptide vaccine delivered by DC-targeting nanoparticles (NPs).

Our lab has established a nano-formulation called lipid-calcium-phosphate (LCP) NPs for delivering nucleic acids, peptides, and chemotherapeutic drugs [13, 14]. The NP core, supported by lipid bilayers, may offer efficient encapsulation and delivery of acid and peptides. Injected NPs must overcome both kinetic and physical barriers after administration. This is especially true for peptides and nucleic acids. After the NP formulation is administered, it must protect the cargo molecules from enzymatic degradation by endogenous nucleases. It should also avoid aggregation, which can be accomplished by PEGylation. The BRAF peptide, along with CpG oligodeoxynucleotides (ODN) adjuvant, was formulated in LCP NPs with mannose modification and delivered to the DCs in the LNs. This approach was very effective in inducing an antigen-specific cytotoxic T lymphocyte (CTL) response in the host and significantly inhibited primary BRAF-mutant melanoma growth. Variations in the extent to infiltrated suppressive leukocytes and T cells within the TME were also monitored after vaccination. The simple but sophisticated LCP NP design is an effective vaccine platform with great translational potential. The BRAF peptide vaccine, which has both MHC-I and HLA-restricted properties, acts as a potent immunotherapy for BRAF-mutant melanoma.

Materials and Methods

Materials

Dioleoylphosphatydic acid (DOPA), (±)-N,N,N-trimethyl-2,3-bis(z-octadec-9-ene-oyloxy)-1-propanaminium chloride (DOTAP), 1,2-distearoyl-sn-glycero-3-phosphoethanolamine-N-[amino(polyethylene glycol)-2000 (DSPE-PEG-2000), and 3-(N-succinimidyloxyglutaryl) aminopropyl, polyethyleneglycol-carbamyl distearoylphosphatidyl-ethanolamine (DSPE-PEG-NHS) were purchased from Avanti Polar Lipids (Alabaster, AL). H-$2D^b$-restricted peptides original $BRAF^{V600E}$ (FGLANEKSI), $BRAF^{WT}$ (FGLANVKSI), modified $BRAF^{V600E}$ peptide (pSpSSFGLANEKSI), and control peptide OVA (SIINFEKL) were purchased from Peptide 2.0 (Chantilly, VA). PEG-DSPE-Mannose was synthesized from DSPE-PEG-NHS and 4-Amino phenyl-mannopyranoside. CpG ODN 1826 (5′-TCCATGACGTTCCTGACGTT-3′) and Cy5-labeled ODN (5′-CAAGGGACTGGAAGGCTGGG-3′) were purchased from Sigma Aldrich (St. Louis, MO).

Cell lines

Murine BRAF-mutant melanoma cell line BPD6 ($BRAF^{V600E}$, $PTEN^{-/-}$, syngeneic with C57BL/6) was obtained from Brent Hanks (Duke Cancer Institute, Durham, NC) and cultivated in RPMI-1640 Medium (Invitrogen, Carlsbad, CA) supplemented with 10% FBS (Invitrogen) and 1% Penicillin/Streptomycin (Invitrogen) at 37 °C and 5% CO_2.

Preparation and Characterization of Vaccine Formulation

The LCP NP was synthesized in a water-in-oil reverse micro-emulsion [15]. Ca phase was formed by mixing 600 µL of 2.5 M $CaCl_2$ with or without peptide and/or CpG ODN in a 20 mL Cyclohexane/Igepal CO-520 (71:29, V:V) solution (oil phase). The oil phase was formed by mixing 600 µL of 12.5 mM Na_2HPO_4 (pH 9.0). We stirred both phases for 5 min then added 400 µL of 20 mM DOPA for 25 min. We then added 40 mL of ethanol and collected cores by centrifugation. Ethanol washes were followed before collection of the cores. Final LCP NPs were formed by mixing 1 mL CaP cores, 100 µL of 20 mM DOTAP, 100 mL cholesterol, 10 mL DSPE-PEG-2000, and 10 µL DSPE-PEG-mannose. After removal of chloroform under reduced pressure, final particles were dispersed in 100 µL of 5% glucose. Transmission electron microscopy (JEOL 100CX II TEM, JEOL, Japan) was used for particle characterization. Particle size and zeta potential were measured with a Malvern Zetasizer Nano ZS in water (Malvern, United Kingdom). DC accumulation of DSPE-PEG-mannose-modified LCP NPs in the draining LNs was investigated by using LCP NPs containing a Cy5-labeled oligonucleotide and flow cytometry analysis of NP uptake in $CD11c^+$ DCs.

Tumor growth inhibition

Female C57BL/6 mice (6–8 weeks old) were purchased from Charles River Laboratories (Wilmington, MA). All animal studies were approved by the IACUC Committee at the University of North Carolina at Chapel Hill (UNC). On day 0, mice were inoculated subcutaneously with 1×10^6 BPD6 cells on their lower flank. Once the tumor volume reached approximately 50 mm^3 ($0.5 \times$ length $\times$ width $\times$ height), mice were then randomized into five groups ($n = 5$–7) as follows: Untreated group (PBS group), Empty LCP NP (Empty group), CpG LCP NPs (CpG group), BRAF LCP NPs (BRAF group), and BRAF + CpG LCP NPs (BRAF + CpG group). Vaccination with LCP NPs was performed on day 10. We monitored tumor size (using digital calipers) and animal weight every 2–3 days. Mice were killed before tumors reached 20 mm in one dimension. At the endpoint, tumors, major organs, and blood samples were harvested and tested. We evaluated anti-tumor efficacy by comparing relative tumor volume (RTV) value and therapeutic group/control group (T/C) ratio. RTV = V_t/V_0, V_t and V_0 represent the tumor volume measured at each time point interval and Day 0. T/C (%) = RTV of therapeutic group/RTV of control group $\times$ 100%. $T/C \leq 42\%$, active, $T/C \leq 10\%$, highly active.

In vivo CTL assay

In vivo CTL was conducted per a previously published protocol [16]. Mice were vaccinated with different formulations on the lower flank. Seven days later, the mice were intravenously injected with a mix of 5×10^6 splenocytes, half of which were pulsed by $BRAF^{V600E}$ peptide (10 µM), while the other half were pulsed by OVA peptide (10 µM). The $BRAF^{V600E}$ pulsed cells were labeled with 4 µM carboxyfluorescein succinimidyl ester (CFSE) and OVA-pulsed cells with 0.4 µM CFSE. These two population were referred to as $CFSE^{high}$ ($BRAF^{V600E}$ pulsed cells) and $CFSE^{low}$ (OVA-pulsed cells). After 18 h, splenocytes were collected and analyzed by flow cytometry. $CFSE^{high}$ and $CFSE^{low}$, as well as in vivo $BRAF^{V600E}$ specific lysis, were calculated [17]. The experiments were conducted in triplicate. Specific lysis was calculated as follows:

$$\%\ \text{Specific lysis} = \frac{\text{OVA} \times x - \text{BRAF}}{\text{OVA} \times x} \times 100$$

where $x = \frac{\text{BRAF}}{\text{OVA}}$ from naive mice.

ELISPOT assay for IFN-γ production

Mice were vaccinated with different formulations of treatment. Seven days later, spleen and draining LNs were collected into single cells and seeded on the capture antibody-coated 96-well plate. IFN-γ production was measured with BD™ ELISPOT assay system (BD Pharmingen, San Diego, CA) as per the manufacturer's instructions [18].

Flow cytometry assay

Immune cell populations were analyzed by flow cytometry. Briefly, tumor tissues or LNs were collected using collagenase A at 37 °C for 40-50 min. Single cells were harvested in PBS and stained with fluorescein-conjugated antibodies. Penetration buffer (BD, Franklin Lakes, NJ) was added for any intracellular cytokine staining.

Immunofluorescence staining

Staining was performed following tissue deparaffinization, antigen retrieval, permeabilization, and BSA blocking. Primary and secondary antibodies conjugated with fluorophores (BD, Franklin Lakes, NJ) were incubated overnight at 4 °C. Cell nuclei were counterstained with DAPI (Vector Laboratories Inc., Burlingame, CA). Images were collected using fluorescence microscopy (Nikon, Tokyo, Japan) and

analyzed using Image J software. Three fields were randomly selected.

TUNEL Assay

Assay performed following DeadEnd Fluorometric TUNEL System (Promega, Madison, WI) instructions [19] and imaged using fluorescence microscopy. Fluorescently stained FITC (green) positives were defined as TUNEL-positive nuclei. Three fields were randomly selected and quantified.

H&E morphology evaluation and blood chemistry analysis

At the endpoint of the tumor inhibition study, mice with different treatments were all subjected to toxicity assays. Both whole blood and serum were collected. We collected and compared whole blood cellular components and tested for indicators of renal and liver function such as creatinine, blood urea nitrogen (BUN), serum aspartate aminotransferase (AST), and alanine aminotransferase (ALT). Organs were collected and send out for H&E staining by UNC histology facility.

Statistical analysis

We used Prism 5.0 software to conduct one-way ANOVA and a two-tailed Student's t test and compared the data with those for the PBS control group. p values less than 0.05 were considered significantly different.

Results

Affinity-modified BRAF peptide was readily packaged in LCP NPs

To achieve more efficient vaccination, we co-delivered NPs encapsulating both the tumor-specific antigen and a potent adjuvant to APCs. CpG ODN, a potent adjuvant, could be efficiently encapsulated in LCP NPs; this system was extensively characterized and optimized in our laboratory [20]. On *N*-terminal of the BRAF peptide, phosphorylated serine residues were designed to facilitate CpG ODN encapsulation. Once the CpG ODN was co-loaded in LCP NPs in a reverse oil-in-water micro-emulsion, amorphous calcium phosphate (CaP) precipitates were formed and then stabilized with DOPA. These so-called CORE particles were then coated with DOTAP/cholesterol and stabilized with DSPE-PEG and DSPE-PEG-mannose. The zeta potential, as determined by a Zetasizer, was approximately 15 mV, which was indicative of full PEGylation of the LCP NPs. Transmission electron microscope (TEM) images were taken to investigate the NP morphology and to confirm the size of the LCP NPs (Fig. 1a–d). The LCP NPs loaded with the modified $BRAF^{V600E}$ peptide and CpG were spherical with a diameter of approximately 30 nm after uranium acetate staining. The encapsulation efficiency was about 60% after optimization. Mannose modification achieved enhanced and prolonged accumulation of the NPs in the LNs, whereas the targeted delivery of NPs to draining LNs facilitated local DC activation ($CD11c^{+}CD86^{+}$), as well as local T cell activation ($CD8^{+}CD69^{+}$), thus boosting immune efficiency (Fig. 1e–f).

BRAF peptide vaccine induced an antigen-specific immune response

We proceeded to evaluate therapeutic efficacy in the murine BRAF-mutant melanoma syngeneic tumor model. CTLs are responsible for killing tumor cells, while IFN-γ-producing T cells secrete cytokines to modulate the TME. Therefore, an assay for antigen-specific CTL response measured how and how well the vaccine formulation worked, whereas assaying IFN-γ-producing T cells measured systemic T cell function upon antigen presentation [16, 18]. LCP NPs loaded with the modified tumor-specific BRAF-mutant peptide were subcutaneously inoculated in the flank of the mice. CTL assay and ELISPOT assay were performed 1 week later to examine the antigen-specific T cell response and IFN-γ production.

As shown in Fig. 2a, immunization with LCP NPs encapsulating the modified BRAF-mutant peptide or CpG ODN alone boosted modest (approximately 48%) efficacy, whereas vaccination with empty particles or NP encapsulating $BRAF^{WT}$ peptide (the wildtype (WT) group) showed no noticeable BRAF-mutant-specific CTL results. Only the combined group with tumor-specific peptide and adjuvant proved effective (approximately 80% efficacy), indicating robust $BRAF^{V600E}$-specific responses.

Moreover, consistent with the CTL assay, we found no significant IFN-γ production of $BRAF^{V600E}$-pulsed cells in the spleens or LNs of naïve mice or empty NP-vaccinated mice, indicating insufficient $BRAF^{V600E}$-specific killing (Fig. 2b). Only full vaccination boosted IFN-γ release. OVA-pulsed or $BRAF^{WT}$-pulsed cells for any group in the spleen or LN also showed no significant IFN-γ production.

Enhanced T cell infiltration into TME results in a superior anti-tumor vaccination effect

The therapeutic efficacy induced by the BRAF peptide vaccine was evaluated in a BRAF-mutant melanoma model. As Fig. 3 shows, this vaccine showed potent tumor growth inhibition compared with other groups. Empty LCP NPs and LCP NPs encapsulating CpG showed no significant therapeutic effect, whereas LCP NPs encapsulating the BRAF

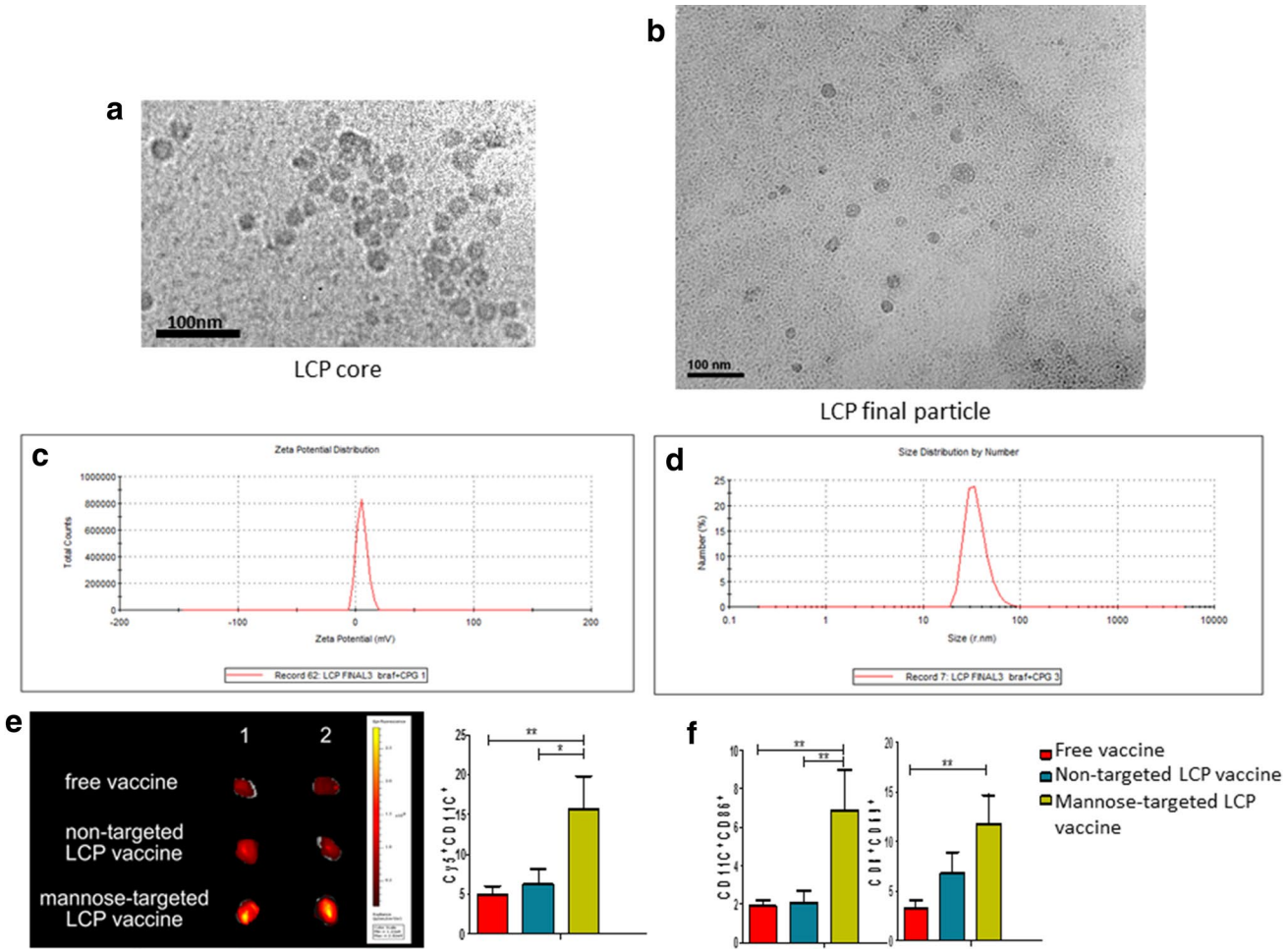

Fig. 1 Characterization of the LCP NP-based BRAF peptide vaccine. LCP encapsulating the modified melanoma-specific antigen ($BRAF^{V600E}$) and adjuvant (CpG ODN) illustrated efficient antigen loading and DC activation. Panels (**a**) and (**b**) show TEM images of NP cores and final structure. Size distribution (**c**) and Zeta potential (**d**) show NP characteristics. Cy5-labeled NPs show enhanced accumulation in draining LNs and uptake in proximal DCs (**e**) after mannose-modified LCP encapsulation, which facilitated local DC activation and T cell activation (**f**). $n = 5$, $^{*}p < 0.05$, $^{**}p < 0.01$

peptide showed modest efficacy, indicating the essential immune function of antigen presenting. Furthermore, the most effective anti-tumor action can only be achieved when using the proper adjuvant. Only the combined full vaccination significantly inhibited tumor growth ($p < 0.01$). Preventive vaccination further reduced melanoma risk. Giving two vaccination dosages (on day 14 and day 7 boosted), the rate of tumor progression decreased significantly; the T/C ratio was 22.3%. Moreover, two out of ten mice achieved tumor-free survival, compared with the PBS control group, suggesting a potential preventive therapy for translational application.

Vaccination's enhanced anti-tumor effect was accompanied by an increase in $CD8^+$ T cell population in the tumors, as determined by both flow cytometry analysis and immunofluorescence staining (Fig. 4). The tumor tissue slices from mice treated with the BRAF peptide vaccine showed extensive T cell infiltration into the tumor region (Fig. 4a). The tumors were further collected and dispersed into single cells. $CD8^+$ T cell ($CD8^+CD45^+$) and T cell activation ($CD8^+CD62L^-$) were analyzed with flow cytometry. The results confirm that the $CD8^+$ T cells significantly increased in number upon activation (Fig. 4b). These data suggest that manipulating the antigen-presenting cells could significantly enhance $CD8^+$ T cell activation and proliferation. The antigen-specific $CD8^+$ T cell killing induced potent cell death within the TME, as indicated by TUNEL assay (Fig. 4c).

Changes of tumor-infiltrating immune cells and collagen within the TME

To further elucidate BRAF peptide vaccination in improving T cell infiltration, we then evaluated the changes of the related immunosuppressive subsets such as Tregs and

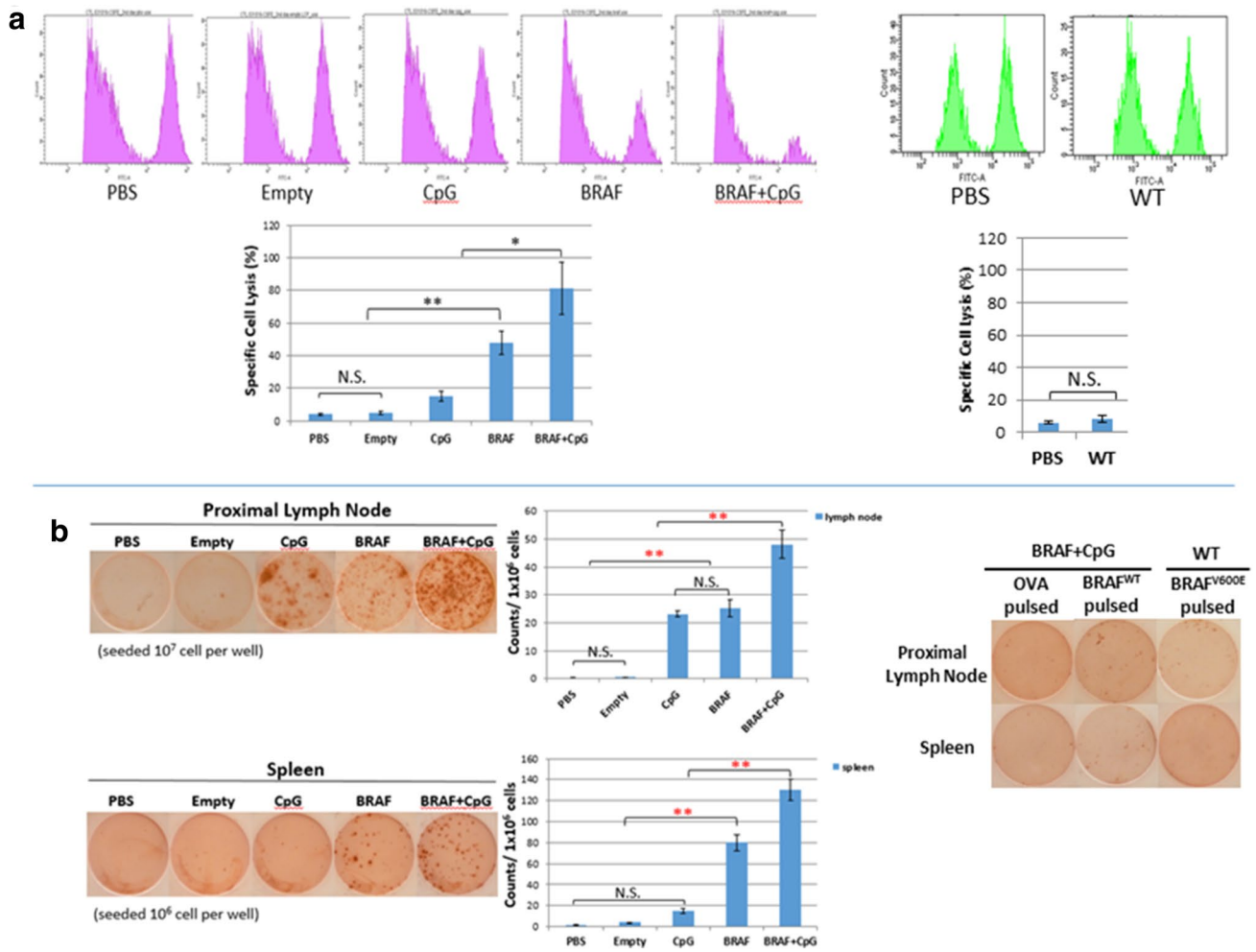

Fig. 2 Antigen-specific immune response induced by the BRAF peptide vaccine. **a** *In vivo* CTL response after vaccination, $n = 5$. **b** IFN-γ production after vaccination was measured with ELISPOT assay system. One representative experiment from each group is shown. $n = 5$, *N.S.* no significance, $*p < 0.05$, $**p < 0.01$

MDSCs, which contributed to a complicated interplay network with $CD8^+$ T cell anti-tumor activity within the collagen-rich BRAF-mutant murine model [21]. The accumulation of these immunosuppressive cells was measured by flow cytometry. As shown in Fig. 5a–b, the percentages of Tregs and MDSCs in the BRAF peptide vaccine group were much lower than in other groups. Macrophages are another important component of the suppressive tumor immune microenvironment. As shown in Fig. 5c, vaccination could efficiently stimulate macrophages to an advantageous tumor-suppressive M1 state. Vaccination significantly increased cytokine production of IFN-γ and IL-4 and decreased anti-inflammatory C–C motif chemokine 2 (CCL2) and IL6 production (Fig. 5e). The BRAF control group alone is insufficient to build up Type 1 T helper (Th1) type immunity. Interestingly, it correlated with increased Tregs and MDSCs. Tumor profiling of cytotoxic T cell ($CD8^+CD45^+$), T cell activation ($CD8^+CD62L^-$), MDSCs ($CD11b^+Gr1^+$), Tregs ($CD4^+Foxp3^+$), and the M1 ($F4/80^+Ly6C^+$) to M2 ($F4/80^+CD206^+$) ratio indicated a strong correlation between high levels of MDSCs and Tregs present in TME with loss of T cell function (activation). Furthermore, a significant decrease in collagen after vaccination indicated a change of the TME morphology that favored further CTL infiltration (Fig. 5f). Although we found no significant increase in infiltrating $CD4^+$ T cells after vaccination (Fig. 5d), there was an overall significant remodeling of the suppressive TME in favor of immunotherapy.

Toxicity evaluation

There was no significant loss in mice body weights, which indicated minor treatment toxicity. No significantly noticeable morphological changes occurred in major organs (Fig. 6). Additionally, serum biochemical value analysis demonstrated normal liver (AST, ALT) and kidney (creatinine,

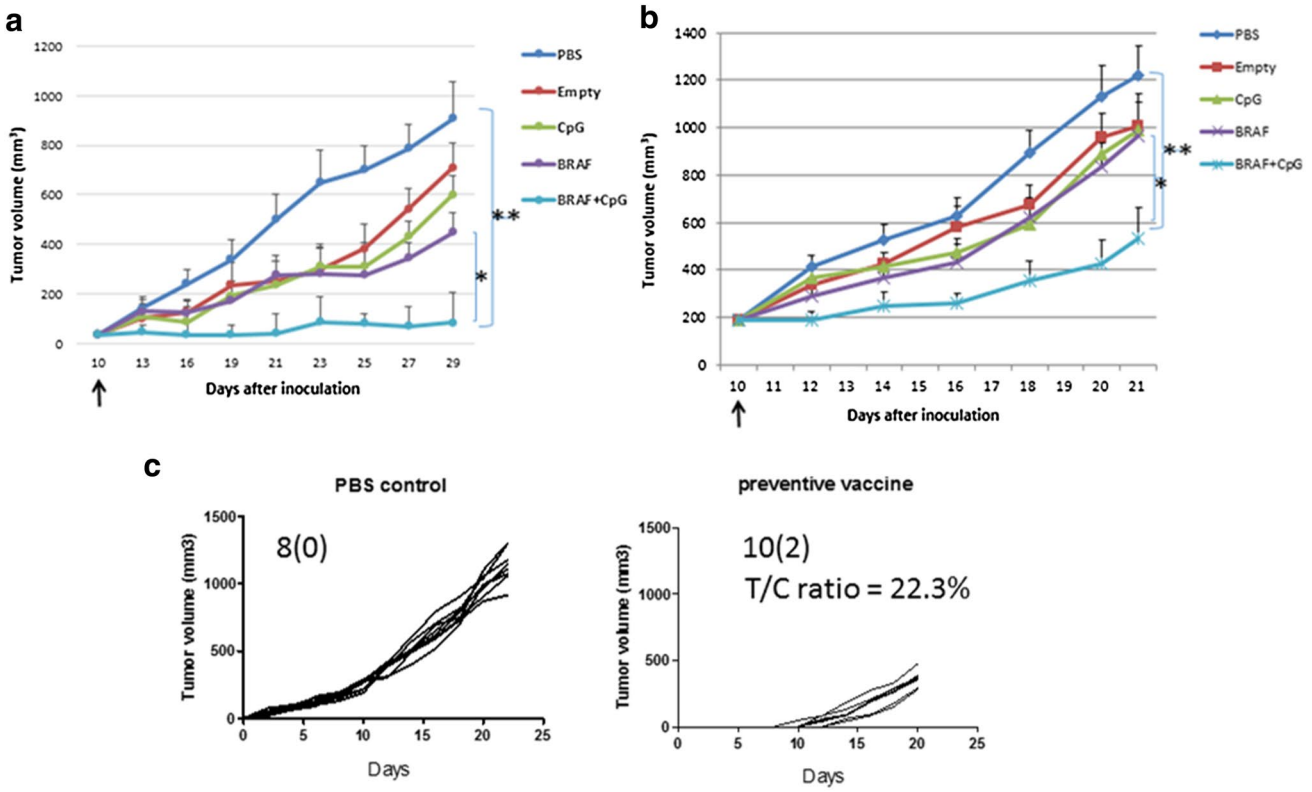

Fig. 3 Anti-tumor activity of the BRAF peptide vaccine in murine BRAF-mutant model. Mice were subcutaneously inoculated with either 2×10^5 (**a**) or 1×10^6 (**b**) BPD6 cells on day 0. Vaccination with 5% glucose (The PBS group), empty LCP (The Empty group), LCP-CpG (The CpG group), LCP-BRAF peptide (The BRAF group), or LCP-(BRAF + CpG) (The BRAF + CpG group) was given on day 10. Tumor growth was measured every 2–3 days. Five mice from each group were killed on day 29, and tumors, whole blood, and organs were harvested for further study. $n = 5$, $^*p < 0.05$, $^{**}p < 0.01$. Preventive vaccination ($n = 10$) significantly reduced tumor growth compared with PBS control ($n = 8$), with T/C ratio of 22.3%. Two animals in the vaccinated group did not grow tumors (**c**)

BUN) function. Whole blood cell counts remained constant within normal ranges for all the groups, suggesting that no systemic anemia or inflammation occurred after treatments.

Discussion and conclusion

Management of advanced melanoma is still a major challenge, and the development of a better understanding of melanoma biology is essential to design new therapeutic strategies and address present challenges associated with existing therapies. In human diseases, over 50% of melanoma cases have corporates BRAF mutations, and approximately, 90% of these mutations are at codon 600. Almost all of these mutations result from a single nucleotide substitution from glutamic acid to valine ($BRAF^{V600E}$) [22]. $BRAF^{V600E}$ results in constitutive kinase pathway activation and unstoppable proliferation [23, 24].

Advanced melanoma is aggressively resistant to chemotherapeutic regimens. Many studies into the molecular basis of melanoma survival and proliferation have identified apoptotic resistance of melanoma cells as the underlying cause of chemo-resistance [25]. This is a formidable challenge for devising treatment strategies for advanced melanoma, and until recently, there was little advancement in standards of care. Dacarbazine has been the sole first-line treatment for melanoma since US Food and Drug Administration (FDA) approved its use in 1976. It has demonstrated a response rate of 10–20% in Phase I and Phase II clinical trials, but overall survival benefit has not been clearly established [26–29]. IFN-α, a type I interferon, is used for adjuvant immunotherapy in advanced melanoma; however, improvements in OS are debatable, and the subset of patients who are sensitive to adjuvant therapy has not been identified [30, 31]. High-dose IL-2 was approved in 1998, but again, the response rate is only about 10% and therapy involves grade 3 toxicities [32].

Immunotherapeutic strategies against melanoma have been extensively investigated in recent years. Tremendous excitement was generated as "checkpoint inhibitors" provided improved OS and disease-free survival over conventional chemotherapy regimens. Ipilimumab, a monoclonal

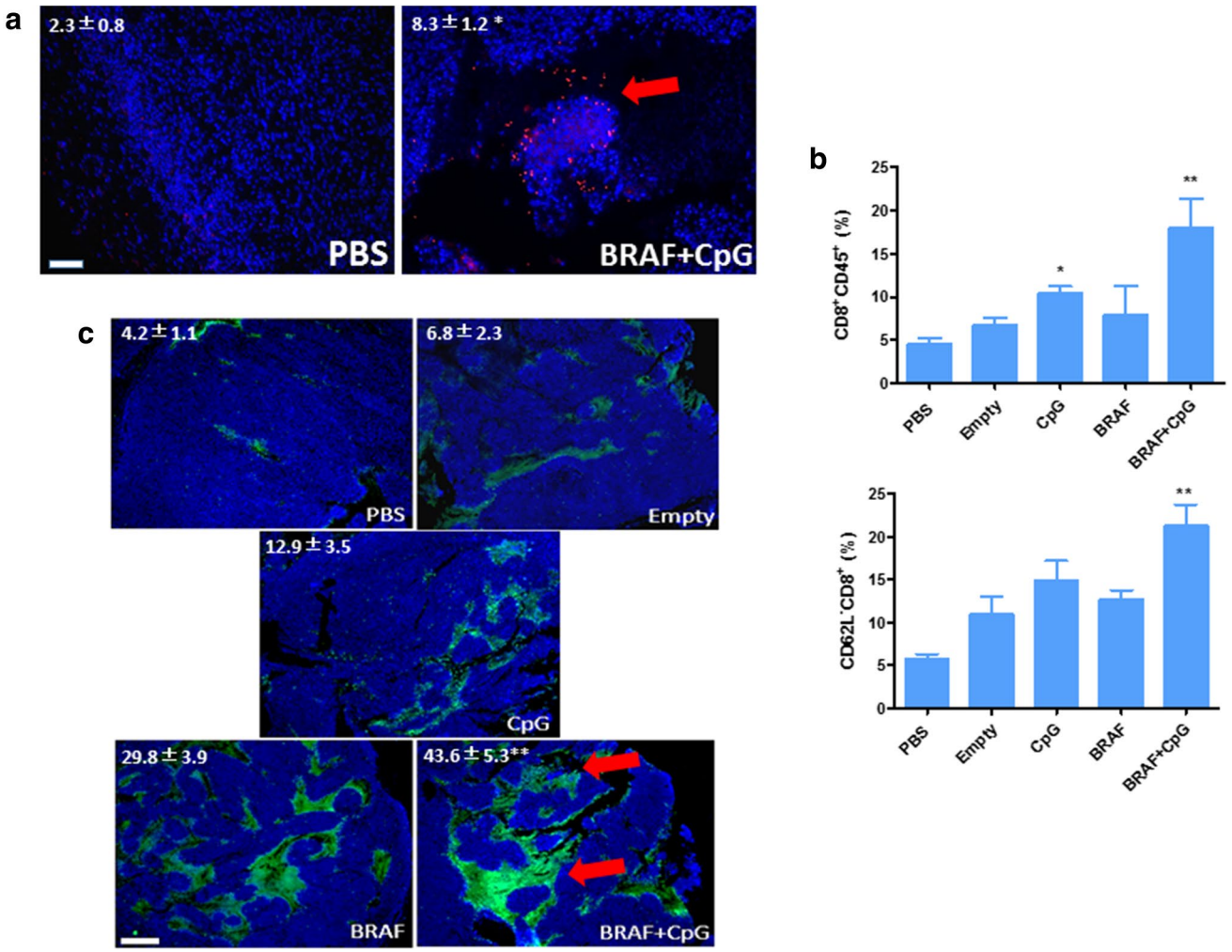

Fig. 4 Enhanced T cell infiltration into tumor microenvironment-induced potent CTL killing. **a** Tissue sections from murine BRAF-mutant model with different treatments were stained for $CD8^+$ (red) and DAPI (blue), then analyzed by immunofluorescence microscopy. Scale bars indicate 200 μm. Arrow indicated infiltrating CTLs. **b** The percentage of $CD8^+$ T cell ($CD8^+CD45^+$) and its activation ($CD8^+CD62L^-$) within tumor regions were quantified by flow cytometry. **c** TUNEL assay indicating apoptotic cell death. Scale bars indicate 300 μm. Arrows indicate apoptotic regions. Numbers in the panel indicate average values of three samples per group, quantified by Image J. $*p < 0.05$, $**p < 0.01$

antibody targeting CTLA-4, received regulatory approval in 2011, followed by pembrolizumab and nivolumab, antibodies against PD-1, in 2014 [33–36]. However, new challenges rapidly emerged as a proportion of patients demonstrated transitory or no responses against checkpoint inhibitors, while long-term survival and even cure were only attained in a small subset of patients [37]. It is thus extremely crucial to identify the right patient subset that may benefit from immunotherapy. However, no biomarker can currently predict clinical outcome [38].

In addition, the TME supported tumor cell survival despite drug exposure and resulted in innate and acquired drug resistance [5, 39]. TME refers to nonmalignant stroma cells that coexist with the neoplastic epithelial cells, including extracellular matrix, cytokines, and growth factors [40]. In addition to initiating multidrug resistance and supporting the tumorigenic process, a permissive microenvironment also acts as a physical barrier that limits the penetration of therapeutic agents, thus inhibiting their anticancer efficacy. Therefore, the complicated nature of the TME suggests that NP-based codelivery of multiple agents for tumor cell-specific targeting and killing may not overcome microenvironment barriers. Combining one regimen targeting and modulating TME-associated drug resistance with another regimen targeting and killing tumor cells holds promise to synergistically improve the therapeutic outcome of cancer treatment [41–43].

In the present work, vaccination using NP delivery effectively treated aggressive growth of BRAF-mutant melanoma. By predicting peptide-MHC class I binding using

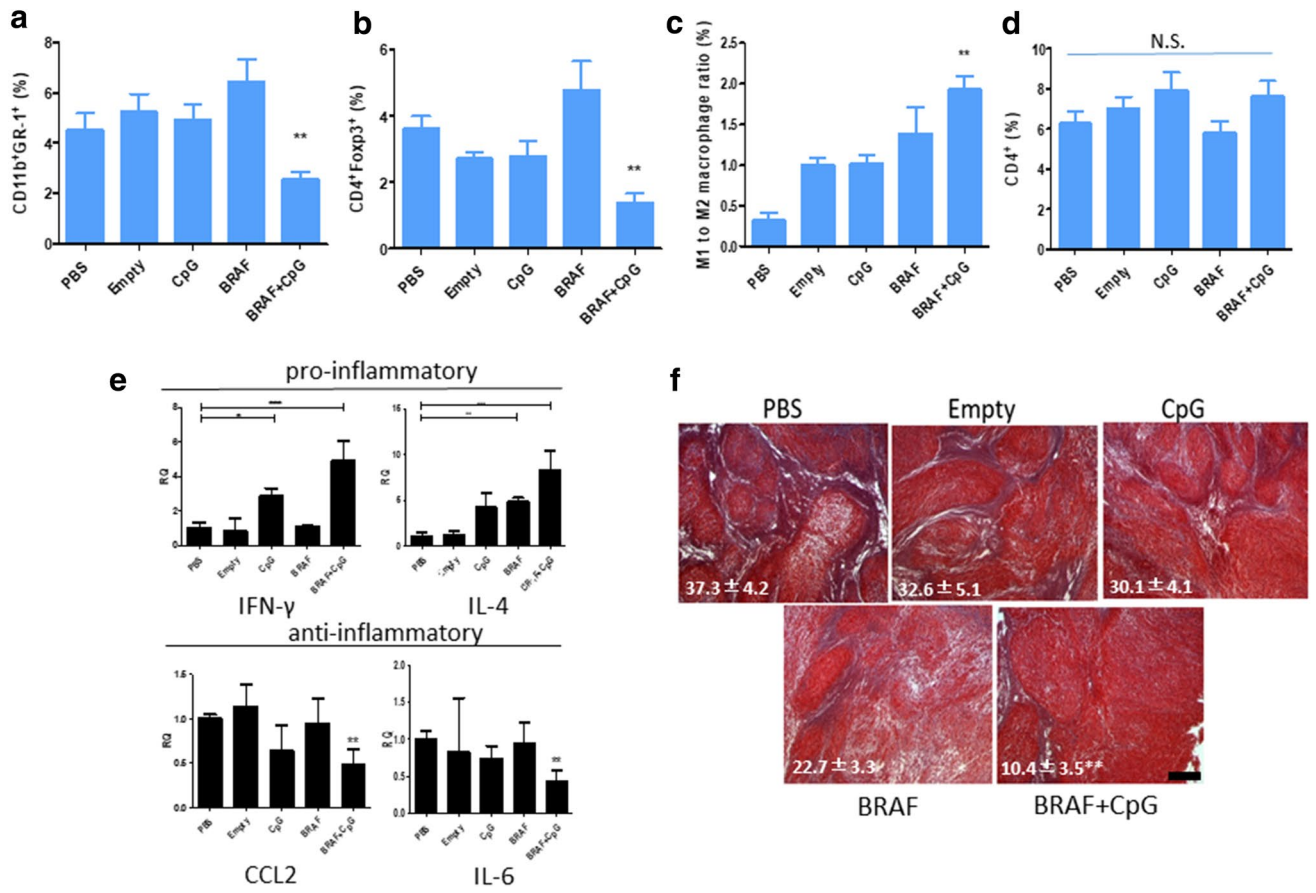

Fig. 5 Change of TME. The percentage of MDSCs (**a**), Treg cells (**b**), M1-to-M2 ratio (**c**), and $CD4^+$ T cells (**d**) within tumor regions were quantified by flow cytometry. Rt-PCR elucidated inflammatory cytokine profile within TME (**e**). Masson's trichrome staining (**f**) indicating change in collagen after different treatments. Numbers in the panel indicate average values of three samples per group, quantified by Image J. $n = 5$. $^*p < 0.05$, $^{**}p < 0.01$. Scale bars indicate 300 μm

artificial neural networks (the NetMHC 4.0 developed by Technical University of Denmark [44, 45]), we identified the murine $BRAF^{V600E}$ peptide FGLANEKSI as a strong binder with binding affinity of 104.92 nM and 0.07% rank (strong binders are defined as having %rank < 0.5, and weak binders with %rank < 2). In vivo studies demonstrated that a single vaccination can induce a strong antigen-specific CTL response and potent tumor growth inhibition for approximately 2 weeks. Again, our LCP NPs provided enhanced vaccination efficacy. LCP, as a $Ca2^+$ reservoir, could effectively modify the intracellular calcium dynamics that drive DC maturation for antigen presentation in a timely manner [46]. This advantage allowed the DCs to orchestrate cytokine production and antigen presentation to induce a potent immune response.

$CD8^+$ T cell-mediated immunity was one crucial mechanism for enhanced anti-tumor immunity [47]. BRAF peptide vaccination induced a local enhancement of tumor-specific T cell infiltration, thus facilitating immune response activation, resulting in a long-term sustained effect. After vaccination, cytotoxic T cells increasingly infiltrated TME derived inflammatory cytokines such as IFN-γ and IL-4 and therefore amplified macrophage polarization. The inflammatory TME facilitated further $Ly6C^+$ monocyte differentiation into M1-like functional phenotypes ($F4/80^+Ly6C^+$). These M1 state macrophages were recruited predominantly to the site of cancer. These key effector cells in the TME boosted local tumor antigen uptake and provided protection against tumor cells. Vaccination, when given at an early stage of tumor progression (tumor volume approximately 50 mm^3 or smaller), would effectively skew immune reactions toward Th1 type. Our data showed a significant decrease in anti-inflammatory cytokines such as CCL2 and IL6. The Th1 type TME promoted effective CTL infiltration rather than activation of Tregs. These cytokine mediators regulated the expansion, migration, and activation of immune suppressive cells in a combinatorial manner. The attraction of CCL2 to MDSCs is well documented [48]. Increased IL6 signaling also promotes MDSCs proliferation once infiltrated. Our vaccine data suggested a potential immunotherapy

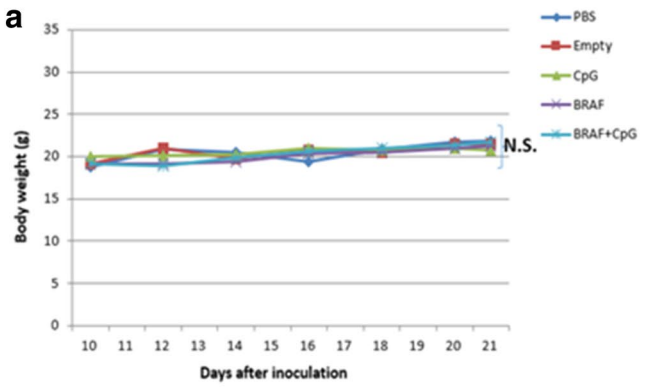

b

	BUN mg/dL	Creatinine mg/dL	AST U/L	ALT U/L
PBS	22.33 ± 1.16	0.26 ± 0.06	215.66 ± 47.5	31 ± 2.65
Empty	26 ± 2.65	0.23 ± 0.06	237.66 ± 11.85	35.66 ± 9.6
BRAF	22.66 ± 4.04	0.2	198 ± 48.7	33.66 ± 4.73
CpG	22.33 ± 1.53	0.2	270.33 ± 82.8	42 ± 8.88
BRAF+CpG	21.33 ± 5.13	0.23 ± 0.06	267 ± 13.2	46.66 ± 6.35
Reference range	8-33	0.2-0.9	54-298	17-132

	WBC(10^3/μL)	HCT(%)	RBC(10^6/μL)	HGB(g/dL)	PLT(10^5/μL)
PBS	10.07 ± 1.56	46.4 ± 0.29	10.01 ± 0.1	15.17 ± 0.29	12.24 ± 2.79
Empty	7.37 ± 0.91	40.53 ± 12.59	8.76 ± 2.92	13.27 ± 4.13	9.73 ± 0.47
BRAF	8.43 ± 1.29	38.1 ± 8.35	8.47 ± 1.53	12.2 ± 2.65	10.73 ± 0.57
CpG	6.83 ± 0.67	46.53 ± 6.42	9.78 ± 0.69	15.2 ± 1.91	11.05 ± 0.79
BRAF+CpG	6.47 ± 1.34	47.73 ± 3.26	9.78 ± 0.45	15.43 ± 1.17	11.59 ± 1.45
Reference range	2.6-10.1	32.8-48	6.5-10.1	10.1-16.1	7.8-15.4

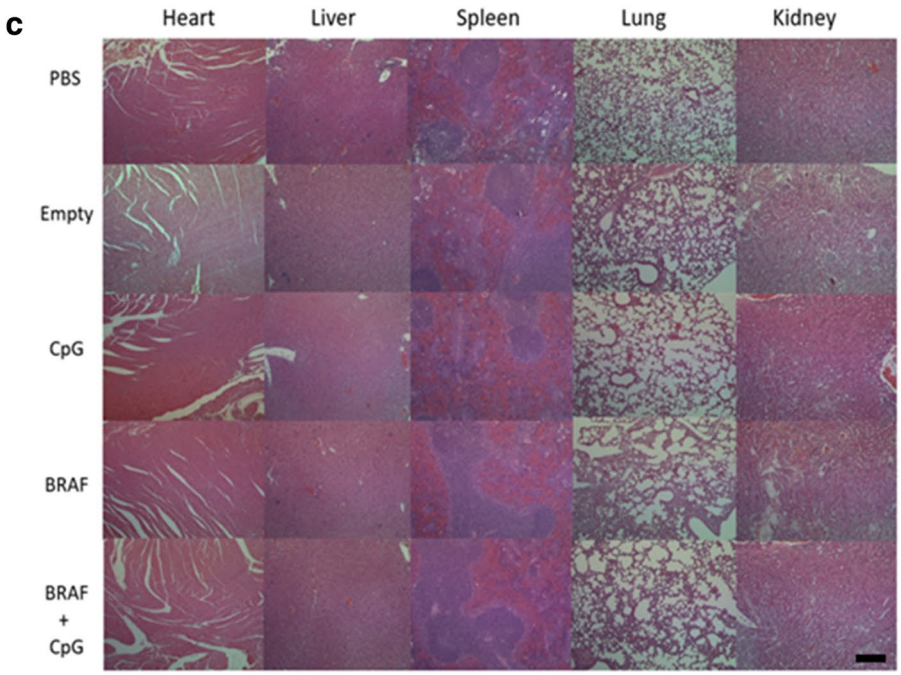

Fig. 6 Safety profile of the BRAF peptide vaccination. **a** Body weights of mice in each group. **b** Whole blood and serum toxicity evaluation. **c** H&E morphology evaluation. The BPD6-bearing mice were divided into five groups with different treatments. Body weights were evaluated every 2–3 days. Mice were euthanized at the endpoint with blood and major organs collected for blood serum and H&E tests. Scale bars indicate 300 μm. $n = 5$. N.S.: $p > 0.05$

by blocking IL6 or CCL2 within TME at an early stage of melanoma progression; we have studies ongoing to test this hypothesis. In addition, for BRAF-mutant melanoma, tumor stroma within immunosuppressive TME supported tumor cell growth. Fibroblast Activation Protein (FAP^+) stroma cells are the major source of collagen production [42, 49]. Our unpublished follow-up work indicates that FAP^+ stroma cells neighboring tumor cells also harbor BRAF mutations and that BRAF vaccination depletes these FAP^+ cells, which improves $CD8^+$ T cells' functions within the TME. Although we found no significant increase in TME infiltrating $CD4^+$ T cells after vaccination, one approach to improve efficacy is to co-load BRAF class II peptides into the same NP delivery system, thereby enhancing the T helper cell memory response. Overall, the modified TME would further enable syngeneic mono-antibody or chemotherapeutic nano-therapy, providing a promising strategy of combining immune therapy with chemotherapy. Thus, targeting TME-changing motifs along with efficient vaccination is a viable future research direction. We are currently working on applying BRAF peptide vaccination on genetically engineered BRAF-mutant murine model, and plan to test this on a humanized murine model.

Dysplastic nevi, also known as unusual-looking benign (noncancerous) moles, are common among Caucasians [50]. These atypical moles greatly increase the risk of developing melanoma, even if there is no family history of melanoma [51]. The BRAF peptide vaccine, which is HLA-restricted,

may thus be developed as a preventive vaccination for use alongside regular exams. Therapeutic vaccines, along with adoptive T cell therapy and CAR-T cell therapy, are some of the novel strategies currently being explored in clinical trials [51, 52]. NPs can thus be potentially exploited as efficient drug-delivery vehicles and may reduce the side effects associated with some of the present therapeutics [53]. Theoretically, NP platforms can be exploited for combinatorial therapy by designing multimodal particles to further clinical translation.

Acknowledgements The work was supported by NIH Grants CA149387 and CA198999. Leaf Huang is a Senior Visiting Scholar of the State Key Laboratory of Molecular Engineering of Polymers, Fudan University, China.

Compliance with ethical standards

Conflict of interest The authors declare that they have no conflict of interest.

References

1. Siegel RL, Miller KD, Jemal A (2016) Cancer statistics, 2016. CA Cancer J Clin 66(1):7–30
2. Gloster HM Jr, Brodland DG (1996) The epidemiology of skin cancer. Dermatol Surg 22(3):217–226
3. Smyth MJ, Dunn GP, Schreiber RD (2006) Cancer immunosurveillance and immunoediting: the roles of immunity in suppressing tumor development and shaping tumor immunogenicity. Adv Immunol 90:1–50
4. Miao L, Li J, Liu Q et al (2017) Transient and local expression of chemokine and immune checkpoint traps to treat pancreatic cancer. ACS Nano 11(9):8690–8706. doi:10.1021/acsnano.7b01786
5. Klemm F, Joyce JA (2015) Microenvironmental regulation of therapeutic response in cancer. Trends Cell Biol 25(4):198–213
6. Sithanandam G, Kolch W, Duh FM et al (1990) Complete coding sequence of a human B-raf cDNA and detection of B-raf protein kinase with isozyme specific antibodies. Oncogene 5(12):1775–1780
7. Chapman PB, Hauschild A, Robert C et al (2011) Improved survival with vemurafenib in melanoma with BRAF V600E mutation. N Engl J Med 364(26):2507–2516
8. Hauschild A, Grob JJ, Demidov LV et al (2012) Dabrafenib in BRAF-mutated metastatic melanoma: a multicentre, open-label, phase 3 randomised controlled trial. Lancet 380(9839):358–365
9. Long GV, Stroyakovskiy D, Gogas H et al (2014) Combined BRAF and MEK inhibition versus BRAF inhibition alone in melanoma. N Engl J Med 371(20):1877–1888
10. Junttila MR, de Sauvage FJ (2013) Influence of tumour microenvironment heterogeneity on therapeutic response. Nature 501(7467):346–354
11. Rammensee H, Bachmann J, Emmerich NP et al (1999) SYFPEITHI: database for MHC ligands and peptide motifs. Immunogenetics 50(3–4):213–219
12. Cintolo JA, Datta J, Xu S et al (2016) Type I-polarized BRAF-pulsed dendritic cells induce antigen-specific CD8 + T cells that impact BRAF-mutant murine melanoma. Melanoma Res 26(1):1–11
13. Guo X, Huang L (2012) Recent advances in nonviral vectors for gene delivery. Acc Chem Res 45(7):971–979
14. Liu Q, Das M, Liu Y et al (2017) Targeted drug delivery to melanoma. Adv Drug Deliv Rev. doi:10.1016/j.addr.2017.09.016
15. Li J, Chen YC, Tseng YC et al (2010) Biodegradable calcium phosphate nanoparticle with lipid coating for systemic siRNA delivery. J Control Release 142(3):416–421
16. Xu Z, Ramishetti S, Tseng YC et al (2013) Multifunctional nanoparticles co-delivering Trp2 peptide and CpG adjuvant induce potent cytotoxic T-lymphocyte response against melanoma and its lung metastasis. J Control Release 172(1):259–265
17. Reddy R, Zhou F, Nair S et al (1992) In vivo cytotoxic T lymphocyte induction with soluble proteins administered in liposomes. J Immunol 148(5):1585–1589
18. Czerkinsky CC, Nilsson LA, Nygren H et al (1983) A solid-phase enzyme-linked immunospot (ELISPOT) assay for enumeration of specific antibody-secreting cells. J Immunol Methods 65(1–2):109–121
19. Chen WS, Xu PZ, Gottlob K et al (2001) Growth retardation and increased apoptosis in mice with homozygous disruption of the Akt1 gene. Genes Dev 15(17):2203–2208
20. Xu Z, Wang Y, Zhang L et al (2014) Nanoparticle-delivered transforming growth factor-beta siRNA enhances vaccination against advanced melanoma by modifying tumor microenvironment. ACS Nano 8(4):3636–3645
21. Lu Y, Miao L, Wang Y et al (2016) Curcumin micelles remodel tumor microenvironment and enhance vaccine activity in an advanced melanoma model. Mol Ther 24(2):364–374
22. Bamford S, Dawson E, Forbes S et al (2004) The COSMIC (Catalogue of Somatic Mutations in Cancer) database and website. Br J Cancer 91(2):355–358
23. Davies H, Bignell GR, Cox C et al (2002) Mutations of the BRAF gene in human cancer. Nature 417(6892):949–954
24. Pratilas CA, Taylor BS, Ye Q et al (2009) (V600E)BRAF is associated with disabled feedback inhibition of RAF-MEK signaling and elevated transcriptional output of the pathway. Proc Natl Acad Sci USA 106(11):4519–4524
25. Soengas MS, Lowe SW (2003) Apoptosis and melanoma chemoresistance. Oncogene 22(20):3138–3151
26. Avril MF, Aamdal S, Grob JJ et al (2004) Fotemustine compared with dacarbazine in patients with disseminated malignant melanoma: a phase III study. J Clin Oncol 22(6):1118–1125
27. Crosby T, Fish R, Coles B et al (2002) Systemic treatments for metastatic cutaneous melanoma. Cochrane Database Syst Rev. doi:10.1002/14651858.CD001215
28. Falkson CI, Ibrahim J, Kirkwood JM et al (1998) Phase III trial of dacarbazine versus dacarbazine with interferon alpha-2b versus dacarbazine with tamoxifen versus dacarbazine with interferon alpha-2b and tamoxifen in patients with metastatic malignant melanoma: an Eastern Cooperative Oncology Group study. J Clin Oncol 16(5):1743–1751
29. Middleton MR, Grob JJ, Aaronson N et al (2000) Randomized phase III study of temozolomide versus dacarbazine in the treatment of patients with advanced metastatic malignant melanoma. J Clin Oncol 18(1):158–166
30. Mocellin S, Pasquali S, Rossi CR et al (2010) Interferon alpha adjuvant therapy in patients with high-risk melanoma: a systematic review and meta-analysis. J Natl Cancer Inst 102(7):493–501
31. Theofilopoulos AN, Baccala R, Beutler B et al (2005) Type I interferons (alpha/beta) in immunity and autoimmunity. Annu Rev Immunol 23:307–336
32. Schwartzentruber DJ, Lawson DH, Richards JM et al (2011) gp100 peptide vaccine and interleukin-2 in patients with advanced melanoma. N Engl J Med 364(22):2119–2127
33. Hodi FS, O'Day SJ, McDermott DF et al (2010) Improved survival with ipilimumab in patients with metastatic melanoma. N Engl J Med 363(8):711–723

34. Robert C, Schachter J, Long GV et al (2015) Pembrolizumab versus ipilimumab in advanced melanoma. N Engl J Med 372(26):2521–2532
35. Hassel JC (2016) Ipilimumab plus nivolumab for advanced melanoma. Lancet Oncol 17(11):1471–1472
36. Wolchok JD, Kluger H, Callahan MK et al (2013) Nivolumab plus ipilimumab in advanced melanoma. N Engl J Med 369(2):122–133
37. Schadendorf D, Hodi FS, Robert C et al (2015) Pooled analysis of long-term survival data from phase II and phase III trials of ipilimumab in unresectable or metastatic melanoma. J Clin Oncol 33(17):1889–1894
38. Topalian SL, Taube JM, Anders RA et al (2016) Mechanism-driven biomarkers to guide immune checkpoint blockade in cancer therapy. Nat Rev Cancer 16(5):275–287
39. Miao L, Guo S, Lin CM et al (2017) Nanoformulations for combination or cascade anticancer therapy. Adv Drug Deliv Rev 115:3–22
40. Nelson CM, Bissell MJ (2006) Of extracellular matrix, scaffolds, and signaling: tissue architecture regulates development, homeostasis, and cancer. Annu Rev Cell Dev Biol 22:287–309
41. Conniot J, Silva JM, Fernandes JG et al (2014) Cancer immunotherapy: nanodelivery approaches for immune cell targeting and tracking. Front Chem 2:105
42. Miao L, Liu Q, Lin CM et al (2017) Targeting tumor-associated fibroblasts for therapeutic delivery in desmoplastic tumors. Cancer Res 77(3):719–731
43. Hu K, Miao L, Goodwin TJ et al (2017) Quercetin remodels the tumor microenvironment to improve the permeation, retention, and antitumor effects of nanoparticles. ACS Nano 11(5):4916–4925
44. Andreatta M, Nielsen M (2016) Gapped sequence alignment using artificial neural networks: application to the MHC class I system. Bioinformatics 32(4):511–517
45. Nielsen M, Lundegaard C, Worning P et al (2003) Reliable prediction of T-cell epitopes using neural networks with novel sequence representations. Protein Sci 12(5):1007–1017
46. Tseng YC, Xu Z, Guley K et al (2014) Lipid-calcium phosphate nanoparticles for delivery to the lymphatic system and SPECT/CT imaging of lymph node metastases. Biomaterials 35(16):4688–4698
47. Medzhitov R, Janeway CA Jr (2002) Decoding the patterns of self and nonself by the innate immune system. Science 296(5566):298–300
48. Umansky V, Sevko A (2013) Tumor microenvironment and myeloid-derived suppressor cells. Cancer Microenviron 6(2):169–177
49. Lo A, Wang LC, Scholler J et al (2015) Tumor-promoting desmoplasia is disrupted by depleting FAP-expressing stromal cells. Cancer Res 75(14):2800–2810
50. Rigel DS, Carucci JA (2005) Malignant melanoma: prevention, early detection, and treatment in the 21st century. CA Cancer J Clin 50(4):215–236 **quiz 237-40**
51. Restifo NP, Dudley ME, Rosenberg SA (2012) Adoptive immunotherapy for cancer: harnessing the T cell response. Nat Rev Immunol 12(4):269–281
52. Porter DL, Levine BL, Kalos M et al (2011) Chimeric antigen receptor-modified T cells in chronic lymphoid leukemia. N Engl J Med 365(8):725–733
53. Allen TM, Cullis PR (2004) Drug delivery systems: entering the mainstream. Science 303(5665):1818–1822